7538–7545 Nucleic Acids Research, 2010, Vol. 38, No. 21 Published online 21 July 2010
doi:10.1093/nar/gkq624

PARP1 suppresses homologous recombination events in mice *in vivo*

Alison Claybon[1,2], Bijal Karia[1,2], Crystal Bruce[3] and Alexander J. R. Bishop[1,2,*]

[1]Greehey Children's Cancer Research Institute, [2]Department of Cellular and Structural Biology, The University of Texas Health Science Center at San Antonio, San Antonio, TX 78229 and [3]Department of Biochemistry and Molecular Biology, Oklahoma State University, Stillwater, OK 74078, USA

Received April 1, 2010; Revised June 27, 2010; Accepted June 28, 2010

ABSTRACT

Recent studies suggest that PARP1 inhibitors, several of which are currently in clinical trial, may selectively kill *BRCA1/2* mutant cancers cells. It is thought that the success of this therapy is based on immitigable lethal DNA damage in the cancer cells resultant from the concurrent loss or inhibition of two DNA damage repair pathways: single-strand break (SSB) repair and homologous recombination repair (HRR). Presumably, inhibition of PARP1 activity obstructs the repair of SSBs and during DNA replication, these lesions cause replication fork collapse and are transformed into substrates for HRR. In fact, several previous studies have indicated a hyper-recombinogenic phenotype in the absence of active PARP1 *in vitro* or in response to DNA damaging agents. In this study, we demonstrate an increased frequency of spontaneous HRR *in vivo* in the absence of PARP1 using the p^{un} assay. Furthermore, we found that the HRR events that occur in *Parp1* nullizygous mice are associated with a significant increase in large, clonal events, as opposed to the usually more frequent single cell events, suggesting an effect in replicating cells. In conclusion, our data demonstrates that PARP1 inhibits spontaneous HRR events, and supports the model of DNA replication transformation of SSBs into HRR substrates.

INTRODUCTION

Poly (ADP-ribosyl)ation is the posttranslational transfer of long chains of negatively charged ADP-ribose moieties to proteins. The resultant increase in negative charge causes the target protein to lose DNA-binding affinity (1). Poly (ADP-ribose) polymerases, or PARPs, comprise a large family of genes that have shared homology with the catalytic domain of the founding member, PARP1 (1). PARP1 has been widely implicated in a multitude of cellular processes including replication (2–4), transcription [reviewed in (5)], chromatin remodeling [reviewed in (5)], telomere maintenance (6) and perhaps most notably, the repair of DNA damage through the base excision repair (BER) pathway (7–9).

Current understanding is that the key BER proteins actually participate in several distinct pathways such as short-patch BER, long-patch BER, single strand break (SSB) repair and nucleotide incision repair (10). However, the common factor for all of these pathways is an SSB—be it the initiating lesion or an intermediate step in a repair process. PARP1 readily binds SSBs (11,12) and recruits the scaffolding protein XRCC1 (13). PARP1 poly (ADP-ribosyl)ates itself (13), reducing its DNA-binding affinity, thus allowing other repair factors to bind the lesion site (9,14).

A recent study demonstrated that chemical inhibition of PARP1 decreased the efficiency of SSB repair (15), conjecturing that chemically inhibited PARP1 remains bound to DNA and blocks other repair proteins from the SSB site. However, the same study revealed that despite PARP1 silencing via RNA interference, cells were able to repair SSBs (15), indicating that an alternative pathway, possibly homologous recombination repair (HRR), can compensate for this loss. Loss of *Parp1* by way of gene targeting in human cells does not hinder formation of nuclear RAD51 foci (an indicator of RAD51-dependent HRR) (16), nor does PARP1 inhibition appear to obstruct HRR *in vitro* (16,17). Waldman and Waldman (18) found a 4-fold increase in intrachromosomal homologous recombination in mouse fibroblasts grown in the poly(ADP-ribose) polymerase inhibitor, 3-methoxybenzamide, compared to controls. Furthermore, PARP1 does not co-localize to RAD51 foci following DNA damage (16) indicating that it is unlikely that PARP1 is directly involved in the HRR process. In addition, increased sister chromatid exchange has been observed with PARP1 inhibitors in Chinese

*To whom correspondence should be addressed. Tel: +1 210 562 9000; Fax: +1 210 562 9014; Email: bishopa@uthscsa.edu

hamster ovary cells (19) and in PARP1 null mice (20), whereas over-expression of *Parp1* decreases the incidence of sister chromatid exchange following DNA damage (21). Resolution of SSBs by way of HRR in the absence of PARP1 activity may be due either to stalled replication fork or DSBs resulting from replication fork collapse. The requirement of such activity is the postulated basis for synthetic lethality observed when treating breast and ovarian cancer cells deficient for either BRCA1 or BRCA2 with PARP1 inhibitors (4,22–24). This is because BRCA1 and BRCA2, amongst their various functions, are required for RAD51 dependent double-stranded DNA break induced HRR (25–27). Together, these *in vitro* observations indicate that loss or inhibition of PARP1 leads to a hyper-recombinogenic phenotype.

Here, we evaluate the spontaneous frequency of HRR *in vivo* using the well-established and highly sensitive p^{un} eye spot assay (28–30). The murine pink-eyed dilution gene, *p*, encodes a protein that functions in the pigmentation of the fur and the retinal pigment epithelium (RPE) of the mouse (31). Mice lacking a functional copy of this gene are hypopigmented, having a dilute (gray) coat and pink eyes (the cells of the RPE are rendered transparent) (31). One such mutant, the 'pink-eyed unstable' (p^{un}) allele contains a 70-kb duplication of exons 6–18 (32–34, Figure 1) and causes this autosomal recessive phenotype. However, the p^{un} allele is subject to a relatively high frequency of spontaneous, somatic reversion to wild-type (35). Reversion can only be attributed to HRR mediated deletion of the duplicated exons, which restores functionality of *p* (32,33) and consequently pigmentation to the fur and RPE. Equivalent assays in yeast have demonstrated that such intrachromosomal deletions between homologous tandem repeats may be mediated by either a RAD51-dependent pathway (canonical HRR pathway) or a RAD51-independent pathway [single strand annealing (SSA), an alternative HRR pathway)] (36). Therefore, the frequency of p^{un} reversion is indicative of the somatic occurrence of spontaneous HRR events (28,29,37). Here we use the p^{un} eye spot assay to demonstrate that the absence of PARP1 results in increased spontaneous somatic HRR events *in vivo*. The significant increase in rare multi-cell clones of eye spots in *Parp1* nullizygous mice suggests that the normal function of PARP1 is to remove DNA lesions prior to their becoming HRR substrates during DNA replication. Our observations substantiate current models of the relationship between PARP1 and HRR, providing formal *in vivo* evidence of a spontaneous, hyper-recombination phenotype.

MATERIALS AND METHODS

Generation of mice

Mice heterozygous for a targeted null allele of *Parp1*, 129S-*Parp1tm1Zqw* (38), were obtained from Jackson Laboratories (Bar Harbor, ME) and genotyped for *Parp1* as described (http://parplink.u-strasbg.fr/protocols/tools/parp1_typing.html) earlier. The $Parp1^{+/-}$ mice were made C57BL/6J congenic by five backcrosses followed by two crosses to C57BL/6J $p^{un/un}$ mice. Mice with homozygous $p^{un/un}$ genotype were selected by their phenotypic gray coat color. The resulting C57BL/6J N7 $Parp1^{+/-}$ $p^{un/un}$ mice (hereafter referred to as $Parp1^{+/-}$) were self-crossed to create the necessary experimental ($Parp1^{-/-}$) and control animals ($Parp1^{+/-}$ and $Parp1^{+/+}$).

P^{un} assay

The p^{un} frequency assay was performed as described earlier (29). Briefly, eyes were harvested, with the investigator blinded to the genotypes until after p^{un} eye spot data was collected. Three types of data were collected for each RPE: the total number of eye spots, the number of cells comprising each eye spot, and the position of each eye spot relative to the optic nerve. Following Bishop *et al.* (29), a p^{un} reversion event or eye spot was defined as 'a pigmented cell or a cluster of pigmented cells, separated by no more than one unpigmented cell'. Eyes were viewed at 15× using a Zeiss Axiovert microscope and methodically scanned for pigmented spots. A 5× mosaic photograph was taken of each RPE using a Zeiss Lumar V.12 stereomicroscope, Zeiss Axiovision MRm camera and Zeiss Axiovision 4.6 software (Thornwood, NY, USA). In cases where a suspected clone consisted of pigmented cells separated by clear cell(s), the Adobe Photoshop CS2 (San Jose, CA, USA) measure tool was used to assess if the unpigmented area between pigmented cells was consistent with the single cell diameter in that part of the RPE (Figure 1). The p^{un} positional assay was then performed as described earlier (28). Briefly, the position of each spot relative to the optic nerve was calculated using simple measurements. In Photoshop, the brush tool was used to mark the approximate center of the optic nerve and the measure tool was then used to obtain two distances for each eye spot: (i) from the center of the optic nerve to the proximal edge of the eye spot, and (ii) from the center of the optic nerve to the edge of the RPE. By dividing the former by the latter, the position of each eye spot relative to the optic nerve was determined.

Primary mouse embryonic fibroblasts and cell culture

Primary mouse embryonic fibroblasts (MEFs) were obtained by intercrossing *Parp1* heterozygous mice to obtain *Parp1* null embryos and littermate controls. Pregnancies were timed by the observation of a vaginal copulation plug and embryos were harvested on Day E14. Embryos were mechanically homogenized and allowed to incubate in 0.05% Trypsin–EDTA for 20 min. Cells were cultured in Dulbecco's modified Eagle's medium supplemented with 10 000 U/ml penicillin, 10 000 μg/ml streptomycin, 25 μg/ml Amphotericin B (Cellgro). The cells were grown at 37°C in the presence of 5% CO_2 in a humidified incubator.

RAD51 nuclear foci immunofluorescence

HRR frequency was determined by immunofluorescence using an antibody against RAD51 (RK-70-005, MBL) as described earlier (39). Cells were grown on acid-washed fibronectin coated cover slips at a density of 1×10^5 cells/cover slip. Cells were then fixed with 4% paraformaldehyde and permeabilized using Triton X-100

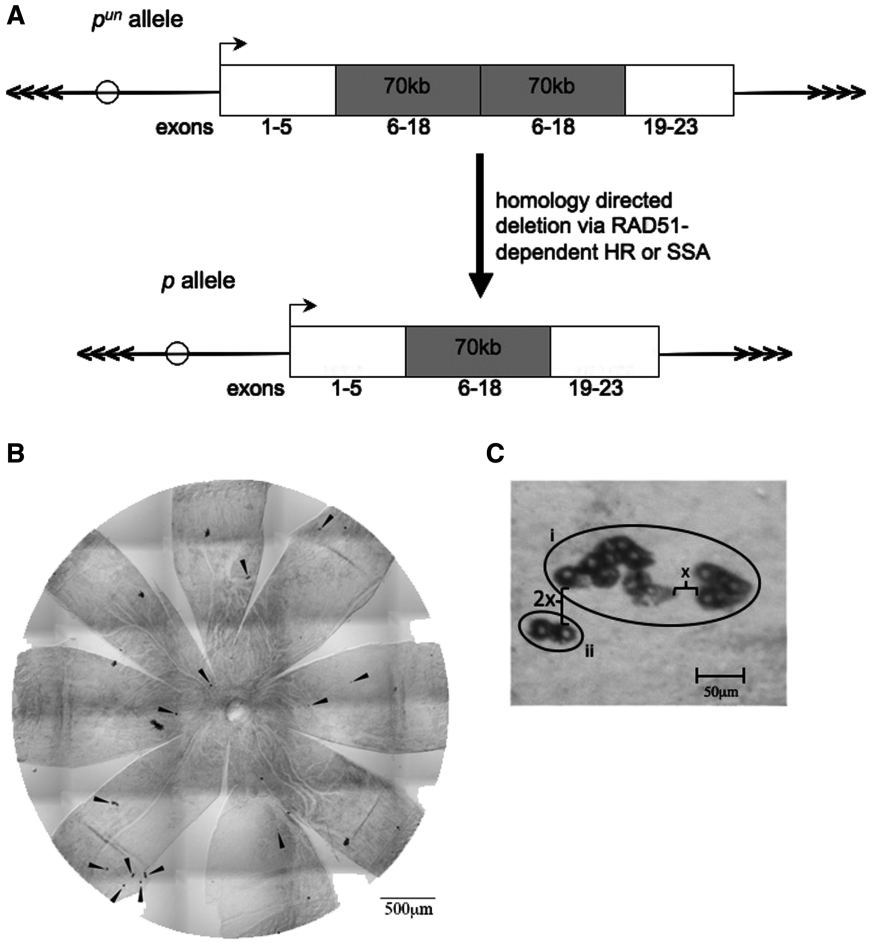

Figure 1. HR-mediated reversion of the p^{un} allele. (**A**) Schematic of the p^{un} mutation. HR events mediate the deletion of one copy of a tandem repeat (of Exons 6–18) rendering the *p* gene functional, thus causing pigmentation of RPE cells. Circles represent centromeres and arrows telomere DNA. (**B**) Mosaic image of a $Parp1^{-/-}$ RPE wholemount. The 13 p^{un} reversion spots are indicated with black arrowheads. (**C**) Example of two distinct p^{un} reversion events within a cluster of pigmented cells. *x* is the diameter of one cell in this region of the RPE and 2× is twice this diameter. For example, the two clusters of cells labeled *i*, are separated by a distance of *x* and are scored as one event. The cluster labeled ii is a distance of 2× from cluster *i*, and therefore represents a distinct event.

for 10 min at room temperature. Blocking was performed with 1% BSA–4% goat serum for 1 h followed by an overnight incubation with RAD51 antibody (1:2000) in a humidified chamber. Goat antichicken Alexa Fluor 488 (Invitrogen) diluted 1:1000 was applied to each cover slip for 1 h followed by DAPI staining and Fluoromount G slide mounting. A minimum of 100 nuclei were examined for each genotype, repeated with three technical replicates per genotype.

Statistics

Parametric analysis of variance was performed in Microsoft Excel 1994 for Mac (Redmond, Washington). The F_{max} test was done by hand per Hartley (40) and Rohlf and Sokal (41). Measurements of skew and kurtosis were obtained using descriptive statistics in Microsoft Excel 1994 for Mac (Redmond, Washington). Non-parametric Kruskal–Wallis test was performed using Stata (College Station, TX, USA). Dunn's test was done by hand per Siegel (42). Chi-squared contingency analysis was performed using the VasserStats online calculator (http://faculty.vasser.edu/lowry/VasserStats.html, accessed 11/2009). Fisher's Exact test (43) was used to compare RAD51 foci quantification using the sum of the technical replicates per genotype.

RESULTS

Loss of *Parp1* leads to a significant increase in HRR *in vivo*

PARP1, amongst its various activities, is involved in SSB repair (11,12). Inhibition of the PARP1 protein in BRCA1 and BRCA2 mutant cells leads to their selective cell death (23,44). This has led to the working model that the observed cell death is due to immitigable DNA damage caused by the loss of two key DNA repair pathways: (i) HRR, due to loss of *BRCA1/2*, and (ii) SSB repair due to inhibition of PARP1 (4,23,24). This model suggests that lack of PARP1 alone will cause an increase in HRR frequency in the absence of exogenous damage. To test this assumption, we determined the spontaneous frequency of

HRR in *Parp1*$^{-/-}$, $^{+/-}$ and $^{+/+}$ animals using the *in vivo* p^{un} assay.

The frequency of p^{un} reversion was determined in *Parp1*$^{-/-}$, $^{+/-}$ and $^{+/+}$ animals using p^{un} eye spot assay (Table 1 and Figure 2). There is a clear increase in the frequency of p^{un} reversion events observed in the absence of PARP1 compared to wild-type and heterozygous littermate controls. Considering that the data is non-parametric and not normal, we used the non-parametric Kruskal–Wallis test (followed by Dunn's test to determine which groups are different from one another). This analysis revealed that *Parp1*$^{-/-}$ animals had a highly statistically significant increase in p^{un} reversion, and thus increased HRR, compared to controls ($P = 0.0001$).

Parp1 null mice have an earlier incidence of p^{un} reversion than controls

The RPE develops radially outward from the optic nerve during development (45), therefore, much like the concentric annual rings of a tree, the positions of eye spots indicate the developmental time at which they occurred (28,29). p^{un} reversion events closer to the optic nerve occurred earlier in development and events further from the optic nerve occurred later in development (29). To investigate whether the increased number of events occurred at a particular time during development, we analyzed the relative positions of the p^{un} reversion events on the RPE of differing *Parp1* genotype (35 wild-type, 28 heterozygous and 24 *Parp1* null RPE). A Kruskal–Wallis test was used to compare the positional distribution of spots and indicated that there is a significant difference between genotypes ($P = 0.0043$, Figure 3). Subsequently, a Dunn's test indicated that the *Parp1* null group is different from the control groups.

To determine whether the difference in the positions of spots was due to early or late events, comparison was done between the numbers of events with proximal positions (earlier in development, 0–0.50) versus the numbers of events with distal positions (later in development, 0.51–1.0). A 2×3 contingency table analysis comparing wild-type, heterozygous and null revealed a highly statistically significant difference in the proportion of spots on the proximal half of the RPE ($\chi^2 = 32.09$, $P < 0.0001$). To verify that the difference was due to the null group, groups were analyzed pairwise. There was no significant difference between wild-type and heterozygous ($P = 0.865$), whereas the null group was significantly different from each of them ($P = 0.005$ and $P = 0.004$, respectively). Finally, 2×2 analysis was performed comparing the null group against the combined heterozygotes and wild-type, confirming a highly statistically significant difference ($\chi^2 = 17.86$, $P < 0.0001$), indicating that there is a shift of p^{un} reversion events to earlier in development. One interpretation of this result is that there is an increased rate of homologous recombination that occurs in the absence of PARP1.

Table 1. Summary of RPE examined and p^{un} reversion frequency by *Parp1* genotype

Genotype	No. of RPE	Total no. of spots	Average no. of spots/RPE	Average spot size (no. cells)
Parp1$^{+/+}$	42	287	6.8	3.5
Parp1$^{+/-}$	34	264	7.8	2
Parp1$^{-/-}$	28	545	19.5	6.2

Clonal expansion of p^{un} reversion events is associated with PARP1 absence

On initial analysis of the RPE, there appeared be a greater number of large (consisting of multiple cells) spots in the *Parp1*$^{-/-}$ RPE (Table 1). Previous studies have shown that spots with greater than 10 cells are very rare (28,30, Bishop, unpublished data). Therefore, a 2×3 contingency table analysis (Chi-square) was computed comparing the number of spots with 10 or fewer cells and the number of spots with 11 or more cells between genotypes ($\chi^2 = 32.65$, $P < 0.0001$, Figure 4). To determine if the null group is

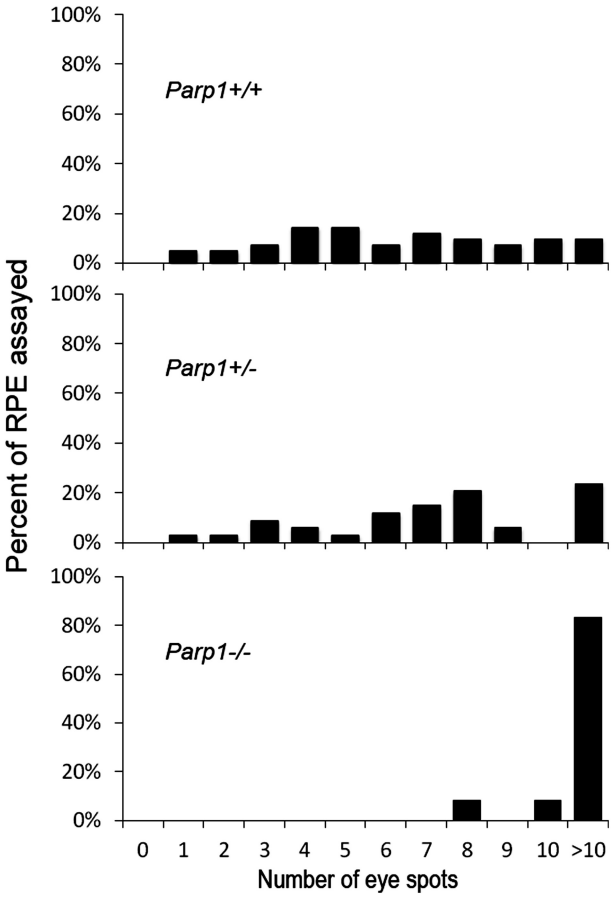

Figure 2. The frequency of p^{un} reversion events in the RPE (pigmented eye spots) in mice with differing *Parp1* genotypes. There is a highly statistically significant difference between the frequency of eye spots in *Parp1*$^{-/-}$ mice compared to wild-type and heterozygous controls ($P = 0.0001$ using the non-parametric Kruskal-Wallis test. A Dunn's test determined that the null group is different from the other two). The *x*-axis is expressed as whole number counts of eye spots, while the *y*-axis is expressed as percent of RPE assayed for that genotype. For example, over 80% of the *Parp1*$^{-/-}$ RPE had greater than 10 eye spots.

Figure 3. Positional distribution of spots in mice with differing *Parp1* genotypes. The position of an eyespot is a measurement relative to the optic nerve head. The position '0', which represents the optic nerve head, correlates to p^{un} reversion events that occurred relatively early in eye development. The position '1', which represents spots at the edge of the RPE, correlates to reversion events that occurred at a later time in eye development. Non-parametric analysis with a Kruskal–Wallis test ($P = 0.013$) followed by a Dunn's Test indicated that there is an increase in HRR more proximal to the optic nerve, and presumably earlier in eye development, in *Parp1* null mice compared to wild-type and heterozygous controls. Wild-type and heterozygous controls showed no difference, so data were combined in this graphical representation to compensate visually for disparity in sample sizes between the null group and either of the controls. The position (along the *x*-axis) and size (along the *y*-axis) of each individual eye spot is represented as a dot. The vertical marker delineates the position that is halfway between the optic nerve head and the edge of the RPE. The horizontal marker represents the divide between large and small eye spots and is therefore at the 11-cell size marker. Any dot on or above this line represents a 'large' eye spot.

the cause of statistical significance and because our frequency and positional analysis showed no difference between wild-type and heterozygous, the data for these two groups were combined and compared against the null group in a 2×2 contingency table analysis ($\chi^2 = 28.64$, $P < 0.0001$). These results indicate that there is a significant increase in the incidence of large spots in the *Parp1* null mice compared to controls, indicating an increase in HRR in proliferating cells.

To investigate whether a particular subset of spots (single cell or multi-cell) caused the observed shift in spots to an earlier time in development in *Parp1* null mice, a Kruskal–Wallis test was used to analyze the relative positions of these subsets of eye spots between genotypes. This test revealed that multi-cell eye spots are shifted toward the optic nerve in the null mice as compared to heterozygous and wild-type ($P = 0.0001$). Furthermore, analysis of the single-cell eye spots showed no difference between groups ($P = 0.5762$, Kruskal–Wallis test), indicating that the positional shift observed when analyzing all spots is in fact due to the multi-cell eye spots. Considering that the *Parp1* null mice display both an increase in the large eye spots and the position of these eye spots, we examined whether these large eye spots are significantly increased in the proximal half of the RPE in the absence of PARP1. A 2×2 contingency table analysis revealed that indeed there was a significant increase in large, multi-cell events ($\geq$11 cells) in the proximal half of the RPE in null mice compared to control RPE ($\chi^2 = 5.49$, $P = 0.019$, Figure 3). This suggests that many more highly replicative cells are prone to p^{un} reversion events during early RPE development in the absence of PARP1.

Loss of *Parp1* leads to an increase in RAD51 nuclear foci

It has been previously reported that human cells either deficient or inhibited for PARP1 have increased RAD51 nuclear foci, an indicator of increased HRR (16,17). To demonstrate that the same cellular phenomenon is observed here with the mouse *Parp1* knockout model, we examined spontaneous levels of RAD51 nuclear foci in MEFs isolated from these mice (Figure 5). As expected, the observed frequency of spontaneous RAD51 foci for wild-type MEFs displayed a very low background, mostly in the category of 0–5 RAD51 foci per cell. However, *Parp1* null MEFs showed a high number of cells with RAD51 foci with 68.3% having >6 foci per cell compared to wild-type MEFs (23.5%) ($P = 2.6e{-}29$). In addition, comparing 0 foci to either the 6–10 or >10 foci per cell groups demonstrates a significant increase in numbers of foci per cell in the *Parp1* null cells ($P = 3.3e{-}15$ and $P = 8.3e{-}25$, respectively). This data suggests a significantly higher frequency of HRR in

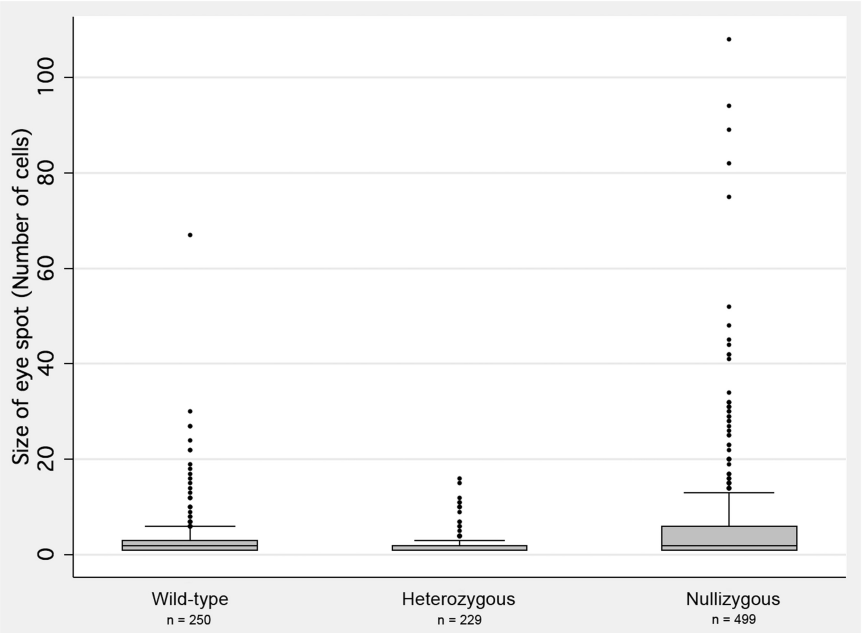

Figure 4. The size of eye spots in mice with differing *Parp1* genotypes**.** Eye spot size is expressed as the number of pigmented RPE cells comprising the eye spot (*y*-axis). A statistically significant increase in the number of large eye spots in *Parp1* null mice ($\chi^2 = 32.65$, $p < 0.0001$) compared to wild-type and heterozygous controls is shown by using a 2×3 contingency table. Comparison of null against combined wild-type and heterozygous data in a 2×2 contingency table also demonstrated a statistically significant difference in the null group ($\chi^2 = 28.64$, $p < 0.0001$).

Parp1 null MEFs compared to wild-type, correlating well with our *in vivo* p^{un} assay observations.

DISCUSSION

The inhibition of PARP1 activity is an exciting novel therapy used in the treatment of BRCA1 and BRCA2 hereditary breast and ovarian cancers (22). The mechanism by which this therapy is thought to work is by synthetic lethality resulting from an inability to repair SSBs by either PARP1-dependent SSB repair or BRCA1/2-dependent HRR (after replication fork stall/ collapse) (4,23,24). This model would suggest an increase in the spontaneous frequency of HRR in the absence of PARP1. *In vitro* evidence for a hyper-recombination phenotype has been presented in various tissue culture experiments (16,17,19–21). Here, we provide *in vivo* evidence that spontaneous HRR frequency is indeed increased in the absence of PARP1 protein by using an established mouse model for measuring HRR events. HRR dependent repair of SSBs has been proposed to be due to DNA replication fork collapse at the SSB that converts these lesions into HRR substrates. Our data supports this notion, with a significant increase in large clonal eye spots in the *Parp1* null background compared to controls. There is no selective advantage for p^{un} reversion, thus it is likely that similar somatic homologous recombination events are occurring in replicating cells throughout all tissues of the body and not just in the developing RPE and at the p^{un} locus.

The p^{un} HRR assay is based on the loss of one copy of a DNA duplication that encompasses exons 6–18 of the

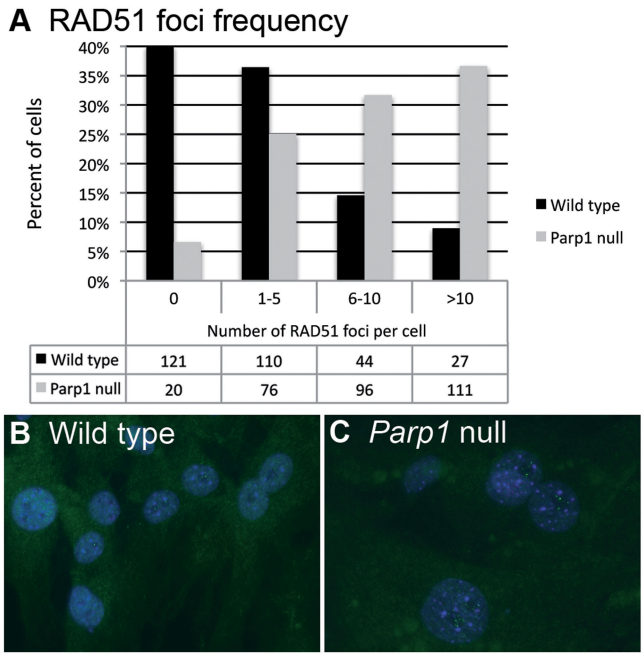

Figure 5. Spontaneous frequency of RAD51 nuclear foci in wild-type and *Parp1* null MEFs. (**A**) Frequency of RAD51 foci per cell by genotype categorized in 0, 1–5, 6–10 and >10 foci by *Parp1* genotype provided as a percentage of cells in the bar graph and actual numbers of cells in the table. There is a statistically significant increase in cells with RAD51 foci in *Parp1* null MEFs compared to wild-type MEFs (comparing 0–5 foci per cell to >6 foci, $P = 2.6e{-}29$). Furthermore, there are more RAD51 foci present per cell in the absence of PARP1. Representative field of cells with RAD51 foci positive cells are presented in (**B**) for wild-type and (**C**) for *Parp1* null MEFs. Blue is DAPI and green is RAD51, taken with a 40× objective.

p gene, restoring the function of this pigmentation gene. Theoretically the p^{un} reversion event, a homology directed deletion, may be mediated by either of two alternative mechanisms (36). First, there is the canonical, RAD51/BRCA1-dependent HRR pathway and is likely instigated by either a double-stranded DNA break or DNA replication fork collapse. The alternative homology-dependent repair pathway is SSA. SSA is a RAD51-independent pathway that can mediate intrachromosomal deletions between homologous DNA sequences, but is unlikely to be dependent upon the DNA replication process and is more likely to act in response to a double-stranded DNA break than an SSB-induced replication fork collapse (46,47). In contrast, RAD51-dependent HRR is considered a high fidelity DNA repair pathway and is likely a favored mechanism in replicating cells. Therefore, RAD51-dependent HRR provides the most obvious explanation for the observation that earlier p^{un} reversion events in proliferating cells will lead to larger eye spots.

Using the p^{un} assay, we previously reported that there is a significant increase in HRR in *Atm*, *p53* and *Gadd45a* null mice compared to controls (28). While these models showed differing shifts in the timing of events (position of eye spots) (28), the distribution of eye spot size was equivalent to wild-type (a majority of single cell eye spots, fewer two cell eye spots, and so forth, Bishop, unpublished data). In contrast, in the *Parp1* null mice we observed a significant increase in the number of multi-cell spots, particularly those greater than 10 cells (Figure 4). It is possible that different HRR pathways are at work in these different mutant mice, with a preference for replication-tied RAD51-dependent HRR events observed in PARP1 null mice.

It has already been postulated that the mechanism by which *Parp1* nullizygosity increases HRR is through replication fork collapse. Therefore, it is probable that it is the RAD51/BRCA1-dependent HRR pathway that results in the hyper-recombination phenotype we have observed in the *Parp1* null animals. In such a case, it would logically follow that more of the spots consist of a greater number of cells because the original cell in which the p^{un} reversion occurred was a proliferating cell; the daughter cells would have inherited the reverted *p* allele and thus will also be pigmented. However, in wild-type, as well as in *Atm*, *p53* and *Gadd45a* null mice, the majority of spots are single-cell events. These events follow the same general pattern of positions as larger spots, but with a phase shift toward the optic nerve. This relative distribution suggests that the single-cell events were likely to have occurred in cells that were in their terminal division at the rear of the proliferating region of the RPE (28). Therefore, it is possible that these single-cell events were not necessarily tied to active replication machinery, but rather could be due to SSA, in a DNA replication-independent manner. BRCA1-dependent HRR is thought necessarily to involve RAD51 (48) yet SSA is thought to be a RAD51-independent event (36). In support of this, we observe a significant increase in spontaneous nuclear RAD51 foci in the absence of PARP1. Though we cannot determine the proportion of p^{un} reversions that result from SSA events, it appears that the absence of PARP1 results in a clear increase in p^{un} reversion events that are tied to cellular proliferation and DNA replication. Overall, our observations provide formal evidence that the absence of PARP1 protein results in a spontaneous hyper-homologous recombination phenotype that supports the proposed mechanisms of PARP1 inhibition and BRCA1/2 null synthetic lethality.

ACKNOWLEDGEMENTS

The authors thank Ting Ting Gu for general technical support and Jo Ann Martinez for helping to establish the mouse lines. The authors also thank members of the Bishop lab for critical reading of the manuscript.

FUNDING

National Institutes of Health (K22ES012264 to A.J.R.B.); US Department of Defense Breast Cancer Research Program Predoctoral Traineeship Award (W81XWH-10-1-0026 to B.K.); Greehey Children's Cancer Research Institute's summer program (to C.B.). Funding for open access charge: Greehey Children's Cancer Research Institute.

Conflict of interest statement. None declared.

REFERENCES

1. Diefenbach,J. and Burkle,A. (2005) Introduction to poly(ADP-ribose) metabolism. *Cell. Mol. Life Sci.*, **62**, 721–730.
2. Simbulan-Rosenthal,C.M., Rosenthal,D.S., Boulares,A.H., Hickey,R.J., Malkas,L.H., Coll,J.M. and Smulson,M.E. (1998) Regulation of the expression or recruitment of components of the DNA synthesome by poly(ADP-ribose) polymerase. *Biochemistry*, **37**, 9363–9370.
3. Dantzer,F., Nasheuer,H.P., Vonesch,J.L., de Murcia,G. and Menissier-de Murcia,J. (1998) Functional association of poly(ADP-ribose) polymerase with DNA polymerase alpha-primase complex: a link between DNA strand break detection and DNA replication. *Nucleic Acids Res.*, **26**, 1891–1898.
4. Bryant,H.E., Petermann,E., Schultz,N., Jemth,A.S., Loseva,O., Issaeva,N., Johansson,F., Fernandez,S., McGlynn,P. and Helleday,T. (2009) PARP is activated at stalled forks to mediate Mre11-dependent replication restart and recombination. *EMBO J.*, **28**, 2601–2615.
5. Kim,M.Y., Zhang,T. and Kraus,W.L. (2005) Poly(ADP-ribosyl)ation by PARP-1: 'PAR-laying' NAD+ into a nuclear signal. *Genes Dev.*, **19**, 1951–1967.
6. d'Adda di Fagagna,F., Hande,M.P., Tong,W.M., Lansdorp,P.M., Wang,Z.Q. and Jackson,S.P. (1999) Functions of poly(ADP-ribose) polymerase in controlling telomere length and chromosomal stability. *Nat. Genet.*, **23**, 76–80.
7. Dantzer,F., Schreiber,V., Niedergang,C., Trucco,C., Flatter,E., De La Rubia,G., Oliver,J., Rolli,V., Menissier-de Murcia,J. and de Murcia,G. (1999) Involvement of poly(ADP-ribose) polymerase in base excision repair. *Biochimie*, **81**, 69–75.
8. Dantzer,F., de La Rubia,G., Menissier-De Murcia,J., Hostomsky,Z., de Murcia,G. and Schreiber,V. (2000) Base excision repair is impaired in mammalian cells lacking Poly(ADP-ribose) polymerase-1. *Biochemistry*, **39**, 7559–7569.
9. Herceg,Z. and Wang,Z.Q. (2001) Functions of poly(ADP-ribose) polymerase (PARP) in DNA repair, genomic integrity and cell death. *Mutat. Res.*, **477**, 97–110.

10. Almeida,K.H. and Sobol,R.W. (2007) A unified view of base excision repair: lesion-dependent protein complexes regulated by post-translational modification. *DNA Rep.*, **6**, 695–711.
11. de Murcia,G. and Menissier de Murcia,J. (1994) Poly(ADP-ribose) polymerase: a molecular nick-sensor. *Trends Biochem. Sci.*, **19**, 172–176.
12. Gradwohl,G., Menissier de Murcia,J.M., Molinete,M., Simonin,F., Koken,M., Hoeijmakers,J.H. and de Murcia,G. (1990) The second zinc-finger domain of poly(ADP-ribose) polymerase determines specificity for single-stranded breaks in DNA. *Proc. Natl Acad. Sci. USA*, **87**, 2990–2994.
13. Masson,M., Niedergang,C., Schreiber,V., Muller,S., Menissier-de Murcia,J. and de Murcia,G. (1998) XRCC1 is specifically associated with poly(ADP-ribose) polymerase and negatively regulates its activity following DNA damage. *Mol. Cell. Biol.*, **18**, 3563–3571.
14. Satoh,M.S. and Lindahl,T. (1992) Role of poly(ADP-ribose) formation in DNA repair. *Nature*, **356**, 356–358.
15. Godon,C., Cordelieres,F.P., Biard,D., Giocanti,N., Megnin-Chanet,F., Hall,J. and Favaudon,V. (2008) PARP inhibition versus PARP-1 silencing: different outcomes in terms of single-strand break repair and radiation susceptibility. *Nucleic Acids Res.*, **36**, 4454–4464.
16. Schultz,N., Lopez,E., Saleh-Gohari,N. and Helleday,T. (2003) Poly(ADP-ribose) polymerase (PARP-1) has a controlling role in homologous recombination. *Nucleic Acids Res.*, **31**, 4959–4964.
17. Yang,Y.G., Cortes,U., Patnaik,S., Jasin,M. and Wang,Z.Q. (2004) Ablation of PARP-1 does not interfere with the repair of DNA double-strand breaks, but compromises the reactivation of stalled replication forks. *Oncogene*, **23**, 3872–3882.
18. Waldman,A.S. and Waldman,B.C. (1991) Stimulation of intrachromosomal homologous recombination in mammalian cells by an inhibitor of poly(ADP-ribosylation). *Nucleic Acids Res.*, **19**, 5943–5947.
19. Oikawa,A., Tohda,H., Kanai,M., Miwa,M. and Sugimura,T. (1980) Inhibitors of poly(adenosine diphosphate ribose) polymerase induce sister chromatid exchanges. *Biochem. Biophys. Res. Commun.*, **97**, 1311–1316.
20. de Murcia,J.M., Niedergang,C., Trucco,C., Ricoul,M., Dutrillaux,B., Mark,M., Oliver,F.J., Masson,M., Dierich,A., LeMeur,M. *et al.* (1997) Requirement of poly(ADP-ribose) polymerase in recovery from DNA damage in mice and in cells. *Proc. Natl Acad. Sci. USA*, **94**, 7303–7307.
21. Meyer,R., Muller,M., Beneke,S., Kupper,J.H. and Burkle,A. (2000) Negative regulation of alkylation-induced sister-chromatid exchange by poly(ADP-ribose) polymerase-1 activity. *Int. J. Cancer*, **88**, 351–355.
22. Fong,P.C., Boss,D.S., Yap,T.A., Tutt,A., Wu,P., Mergui-Roelvink,M., Mortimer,P., Swaisland,H., Lau,A., O'Connor,M.J. *et al.* (2009) Inhibition of poly(ADP-ribose) polymerase in tumors from BRCA mutation carriers. *N Engl. J. Med.*, **361**, 123–134.
23. Farmer,H., McCabe,N., Lord,C.J., Tutt,A.N., Johnson,D.A., Richardson,T.B., Santarosa,M., Dillon,K.J., Hickson,I., Knights,C. *et al.* (2005) Targeting the DNA repair defect in BRCA mutant cells as a therapeutic strategy. *Nature*, **434**, 917–921.
24. Turner,N., Tutt,A. and Ashworth,A. (2005) Targeting the DNA repair defect of BRCA tumours. *Curr. Opin. Pharmacol.*, **5**, 388–393.
25. Bhattacharyya,A., Ear,U.S., Koller,B.H., Weichselbaum,R.R. and Bishop,D.K. (2000) The breast cancer susceptibility gene BRCA1 is required for subnuclear assembly of Rad51 and survival following treatment with the DNA cross-linking agent cisplatin. *J. Biol. Chem.*, **275**, 23899–23903.
26. Moynahan,M.E., Chiu,J.W., Koller,B.H. and Jasin,M. (1999) Brca1 controls homology-directed DNA repair. *Mol. Cell.*, **4**, 511–518.
27. Moynahan,M.E., Pierce,A.J. and Jasin,M. (2001) BRCA2 is required for homology-directed repair of chromosomal breaks. *Mol. Cell.*, **7**, 263–272.
28. Bishop,A.J., Hollander,M.C., Kosaras,B., Sidman,R.L., Fornace,A.J. Jr and Schiestl,R.H. (2003) Atm-, p53-, and Gadd45a-deficient mice show an increased frequency of homologous recombination at different stages during development. *Cancer Res.*, **63**, 5335–5343.
29. Bishop,A.J., Kosaras,B., Carls,N., Sidman,R.L. and Schiestl,R.H. (2001) Susceptibility of proliferating cells to benzo[a]pyrene-induced homologous recombination in mice. *Carcinogenesis*, **22**, 641–649.
30. Bishop,A.J., Kosaras,B., Sidman,R.L. and Schiestl,R.H. (2000) Benzo(a)pyrene and X-rays induce reversions of the pink-eyed unstable mutation in the retinal pigment epithelium of mice. *Mutat. Res.*, **457**, 31–40.
31. Brilliant,M.H. (2001) The mouse p (pink-eyed dilution) and human P genes, oculocutaneous albinism type 2 (OCA2), and melanosomal pH. *Pigment Cell Res.*, **14**, 86–93.
32. Brilliant,M.H., Gondo,Y. and Eicher,E.M. (1991) Direct molecular identification of the mouse pink-eyed unstable mutation by genome scanning. *Science*, **252**, 566–569.
33. Gondo,Y., Gardner,J.M., Nakatsu,Y., Durham-Pierre,D., Deveau,S.A., Kuper,C. and Brilliant,M.H. (1993) High-frequency genetic reversion mediated by a DNA duplication: the mouse pink-eyed unstable mutation. *Proc. Natl Acad. Sci. USA*, **90**, 297–301.
34. Oakey,R.J., Keiper,N.M., Ching,A.S. and Brilliant,M.H. (1996) Molecular analysis of the cDNAs encoded by the pun and pJ alleles of the pink-eyed dilution locus. *Mamm. Genome*, **7**, 315–316.
35. Melvold,R.W. (1971) Spontaneous somatic reversion in mice. Effects of parental genotype on stability at the p-locus. *Mutat. Res.*, **12**, 171–174.
36. Ira,G. and Haber,J.E. (2002) Characterization of RAD51-independent break-induced replication that acts preferentially with short homologous sequences. *Mol. Cell. Biol.*, **22**, 6384–6392.
37. Bodenstein,L. and Sidman,R.L. (1987) Growth and development of the mouse retinal pigment epithelium. II. Cell patterning in experimental chimaeras and mosaics. *Dev. Biol.*, **121**, 205–219.
38. Wang,Z.Q., Auer,B., Stingl,L., Berghammer,H., Haidacher,D., Schweiger,M. and Wagner,E.F. (1995) Mice lacking ADPRT and poly(ADP-ribosyl)ation develop normally but are susceptible to skin disease. *Genes Dev.*, **9**, 509–520.
39. Busuttil,R.A., Munoz,D.P., Garcia,A.M., Rodier,F., Kim,W.H., Suh,Y., Hasty,P., Campisi,J. and Vijg,J. (2008) Effect of Ku80 deficiency on mutation frequencies and spectra at a LacZ reporter locus in mouse tissues and cells. *PLoS ONE*, **3**, e3458.
40. Hartley,H.O. (1950) The use of range in analysis of variance. *Biometrika*, **37**, 271–280.
41. Rohlf,F.J. and Sokal,R.R. (1995) *Statistical Tables*, 3rd edn. Freeman and Company, New York.
42. Siegel,S. and Castellan,N.J. (1956) *Non-Parametric Statistics for Behavioral Sciences*. McGraw Hill, New York.
43. Fisher,R. (1922) On the interpretation of $\chi 2$ from contingency tables, and the calculation of P. *J. Roy. Statist. Soci.*, **85**, 87–94.
44. Bryant,H.E., Schultz,N., Thomas,H.D., Parker,K.M., Flower,D., Lopez,E., Kyle,S., Meuth,M., Curtin,N.J. and Helleday,T. (2005) Specific killing of BRCA2-deficient tumours with inhibitors of poly(ADP-ribose) polymerase. *Nature*, **434**, 913–917.
45. Bodenstein,L. and Sidman,R.L. (1987) Growth and development of the mouse retinal pigment epithelium. I. Cell and tissue morphometrics and topography of mitotic activity. *Dev. Biol.*, **121**, 192–204.
46. Galli,A. and Schiestl,R.H. (1998) Effect of Salmonella assay negative and positive carcinogens on intrachromosomal recombination in S-phase arrested yeast cells. *Mutat. Res.*, **419**, 53–68.
47. Galli,A. and Schiestl,R.H. (1998) Effects of DNA double-strand and single-strand breaks on intrachromosomal recombination events in cell-cycle-arrested yeast cells. *Genetics*, **149**, 1235–1250.
48. Cousineau,I., Abaji,C. and Belmaaza,A. (2005) BRCA1 regulates RAD51 function in response to DNA damage and suppresses spontaneous sister chromatid replication slippage: implications for sister chromatid cohesion, genome stability, and carcinogenesis. *Cancer Res.*, **65**, 11384–11391.